Electromagnetics and Antenna Technology, Ch. 10

Alan J. Fenn

Senior Staff Member
Lincoln Laboratory
Massachusetts Institute of Technology
244 Wood Street
Lexington, MA 02420

July 6, 2017

This material is based upon work supported under Air Force Contract No. FA8721-05-C-0002 and/or FA8702-15-D-0001. Any opinions, findings, conclusions or recommendations expressed in this material are those of the author(s) and do not necessarily reflect the views of the U.S. Air Force.

10

Design and Analysis of a Planar Array-Fed Axisymmetric Gregorian Reflector System

10.1 Introduction

In this chapter, an axisymmetric array-fed confocal parabolic Gregorian reflector antenna system for potential deployment in space from a small satellite is explored. The antenna utilizes a planar array located near the vertex of the primary parabolic reflector. Electromagnetic simulations are used to analyze and optimize the antenna parameters for fixed on-axis peak directivity performance. Simulations of the radiation pattern performance of a dual reflector system with an electrically large primary and small subreflector and high magnification are presented. The chapter is organized as follows. Section 10.2 describes the antenna design. Section 10.3 shows simulated results. Section 10.4 has a summary.

10.2 Antenna Design

Reflector antennas are of interest for space applications requiring high gain and low sidelobes. In the case of a space-deployable antenna, a reduction in mass is an important goal, which might be achieved using inflatable structures which have been investigated by a number of researchers [1–7]. In the present chapter, an axisymmetric reflector antenna design is described, which is depicted as an artist's concept in Figure 10.1. It is assumed here that a satellite has accurate attitude control pointing so that errors in the antenna main beam pointing direction can be neglected. A thin-profile planar array would be

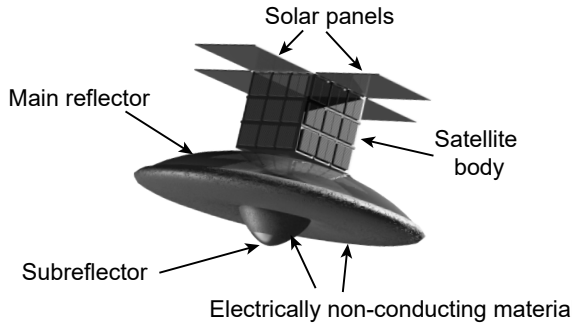

Figure 10.1 Artist depiction of a concept for an inflatable axisymmetric dual-reflector antenna deployed from a satellite.

located near the vertex of the main reflector and attached to the satellite body. An example offset Gregorian reflector antenna system with a planar phased array feed was shown previously in Chapter 2, Figure 2.13. However, here an axisymmetric Gregorian antenna system design with confocal paraboloids and planar array feed was desired, which could allow easier fabrication and inflatable deployment compared to an offset Gregorian or Cassegrain design [8–11]. Limited electronic scanning with an axisymmetric Gregorian dual reflector with confocal paraboloids and a planar phased array feed has been demonstrated by simulations [12]. Thin-film materials with and without electrically conducting coatings can be considered for designing an inflatable space-deployable antenna [13–16]. An ideal planar array source feeding the Gregorian subreflector is assumed in the simulations that follow. In the case where the large primary reflector surface could have distortion that creates phase errors, a phased array feed could provide phase compensation. When a large focal magnification is used in the Gregorian design, the blockage of the main beam by the subreflector can be relatively small. The primary reflector diameter is assumed here to be 2.4m with an ideal (undistorted) surface operating at Ku-band at 16 GHz ($\lambda = 1.875$ cm). With this electrically large aperture (128λ at 16 GHz), the antenna system has been analyzed and optimized using sparse moment method simulations with the multilevel fast multipole method (MLFMM) [10, pp. 209–253, 11].

Figure 10.2 shows a side view of a general axisymmetric Gregorian antenna with confocal parabolic reflectors. The common focal point is located close to the subreflector along the axis of both reflectors. The primary reflector has a diameter D and a focal distance f_p. The subreflector has a diameter d and a focal distance f_s. In Figure 10.3, ray paths are shown for the case where a field is incident along the axial direction of the reflector system. In general, a ray incident on the reflector surface will have the reflected angle equal to the

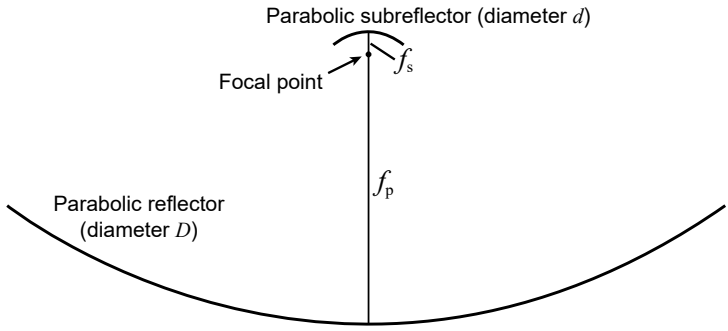

Figure 10.2 Side view of an axisymmetric Gregorian antenna with confocal parabolic reflectors.

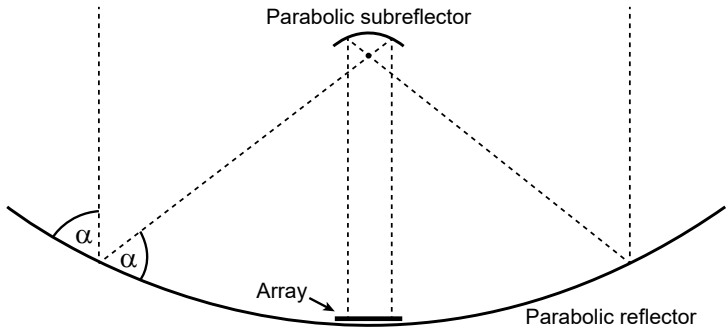

Figure 10.3 Side view of an array-fed axisymmetric Gregorian antenna with confocal parabolic reflectors and ray paths shown as dashed lines.

incident angle. Since the subreflector and primary reflector are confocal, the ray path from the subreflector to the array is also in the axial direction. Thus, a uniform plane wave with constant amplitude and phase distribution received across the aperture of the primary reflector will be received at the planar array with constant amplitude and phase distribution.

As described by Fitzgerald [9], the magnification factor m for the Gregorian dual-reflector antenna system with confocal paraboloids is given by the ratio of the primary to subreflector focal distances or

$$m = f_p / f_s \tag{10.1}$$

In the case where limited main beam scanning from the Gregorian antenna system boresight would be desired, the array would need to be phased such that the array scan angle θ_{sa} is, to first order, equal to the Gregorian main

beam scan angle θ_{sg} times the magnification factor m. That is,

$$\theta_{sa} = m\theta_{sg} \tag{10.2}$$

In the limited scanning case, as Fitzgerald has described, the phased array location relative to the location of the subreflector is a significant design parameter. Additionally, as the array scan angle increases the subreflector must be oversized to avoid significant spillover, otherwise the Gregorian main beam gain would decrease and the sidelobe levels would increase. However, in this chapter only the fixed-boresight case is examined.

As shown in Figure 10.4, an example fixed-boresight Ku-band Gregorian confocal reflector system with a primary parabolic reflector diameter D=2.4m and focal distance $f_p = 0.9$m ($f_p/D = 0.375$), parabolic subreflector diameter $d = 0.25$m and focal distance $f_s = 0.08$m ($f_s/d = 0.32$), and planar array diameter 0.2m, has been analyzed and optimized using numerical simulations conducted with the FEKO software (www.feko.info) MLFMM solver. The

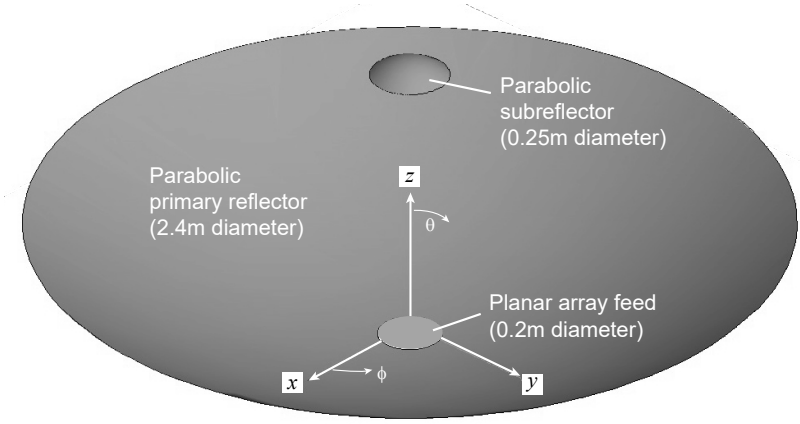

Figure 10.4 Simulation model for the axisymmetric Gregorian antenna with confocal parabolic reflectors and planar array feed.

feed array geometry is depicted in Figure 10.5. The 20 cm diameter array feed was modeled in FEKO as a near-field source that approximates a uniformly illuminated planar array of 140 ideal Hertzian (short) electric dipoles polarized in the y direction. For this feed, the array elements are assumed to be spaced on a truncated square lattice with element spacing 1.5 cm which corresponds to 0.8λ at 16 GHz.

The primary and secondary reflectors were analyzed as perfect electric conductors with ideal parabolic shape. Optimization was performed as a grid search with the subreflector diameter d and subreflector focal distance f_s taken

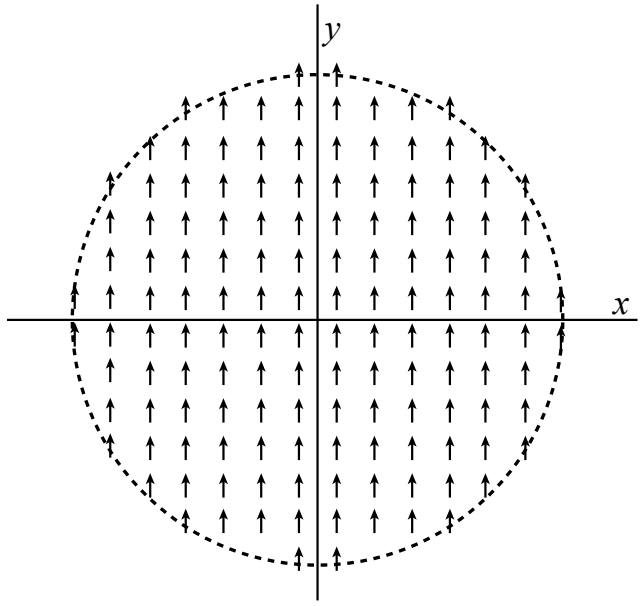

Figure 10.5 Aperture excitation model for the 20 cm diameter planar array feed.

as the search parameters. The search optimization goal was assumed here to be peak directivity at boresight. The magnification factor m for this dual-reflector antenna system is given by the ratio of the primary to subreflector focal distances from Equation (10.3) as

$$m = f_p/f_s = 11.25 \tag{10.3}$$

The angle from the center of the feed array to the edge of the subreflector is approximately 8°.

10.3 Electromagnetic Simulation Results

The dual-reflector Gregorian reflector system was simulated with 3,810,646 moment method basis functions using the FEKO fast multipole method on a computer system utilizing 34 parallel processors on two CPUs at 2.3 GHz. The peak memory usage was 5.2 GBytes and the execution time was 392 seconds. The simulated far-field (infinite range) and near-field (range 0.98m at the subreflector) radiation patterns of the uniformly illuminated 20-cm diameter planar array feed are shown in Figure 10.6. The far-field radiation pattern of the array feed has nulls formed at $\pm 6.5^\circ$ and the first sidelobes

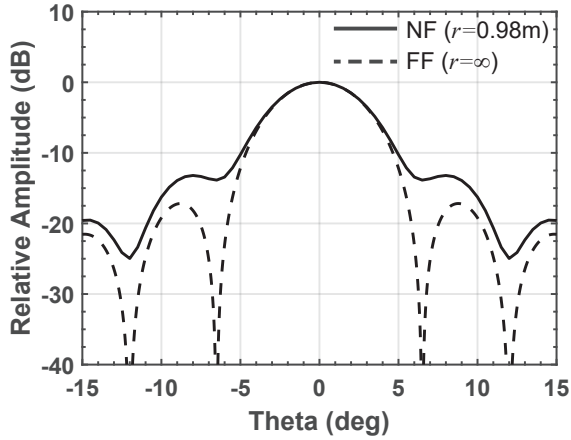

Figure 10.6 Comparison of the simulated near field (range is 0.98m) and far field (infinite range) radiation patterns of the planar array feed. The angle formed from the center of the feed array to the edge of the subreflector is $\pm 8^{\circ}$.

are at the -18.2 dB level. In contrast, the feed array near-field amplitude at range distance 0.98m that illuminates the edge of the subreflector is at the -13.2 dB level (edge illumination) and the far-field null at $\pm 6.5^{\circ}$ is filled in at the -13.8 dB level.

The simulated two-dimensional near-field radiation pattern for the electric-field y component in the xz plane at $y = 0$ of the Gregorian reflector system is shown in Figure 10.7. In Figure 10.7, with the array feed operating

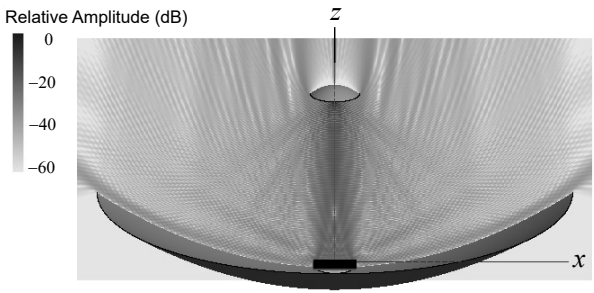

Figure 10.7 Simulated two-dimensional near-field radiation pattern of the Gregorian reflector system.

in transmit mode the field is concentrated toward the subreflector, and blockage by the subreflector is observed in the near field amplitude behind

the subreflector. The simulated surface currents on the subreflector and primary reflector are depicted in Figure 10.8. The surface current magnitude is

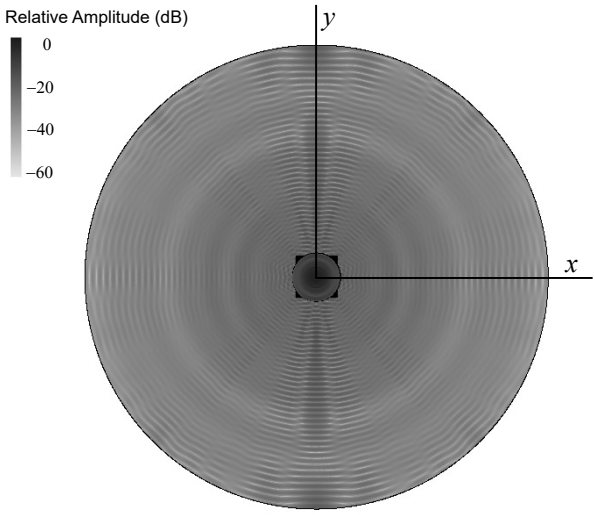

Figure 10.8 Simulated surface current density on the subreflector and primary reflector of the Gregorian reflector system.

observed to be centered and concentrated on the subreflector. The simulated E-plane and H-plane directivity patterns for the Gregorian reflector system over a $\pm 15^{\circ}$ field of view at 16 GHz are shown in Figure 10.9. The simulated radiation pattern characteristics are as follows: peak directivity is 49.4 dBi, half-power beamwidth is 0.52°, and first sidelobe level is -28.5 dB. For a 2.4 meter diameter aperture with 100% efficiency, the peak directivity at 16 GHz is 52 dBi, so the simulated aperture efficiency of this antenna design is 55%.

10.4 Summary

An axisymmetric array-fed confocal parabolic Gregorian reflector antenna system for potential inflatable deployment in space from a small satellite has been analyzed. The antenna utilizes a planar array located near the vertex of the primary parabolic reflector. Electromagnetic simulations based on the multilevel fast multipole method were used to analyze and optimize the antenna parameters for fixed on-axis peak directivity performance. Simulations of the radiation pattern performance of this dual-reflector system with a 2.4m diameter primary reflector operating at Ku band indicate that high gain and low sidelobes can be achieved with this design approach. All

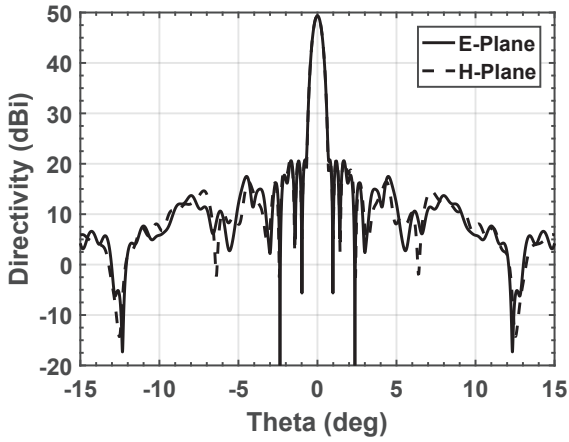

Figure 10.9 Comparison of the simulated E-plane and H-plane directivity patterns for the planar array fed axisymmetric Gregorian reflector system at 16 GHz

.

of the results presented in the chapter assumed ideal aperture illumination and ideal parabolic surfaces for the primary and secondary reflectors. Future work in this area could consider the effects of reflector surface distortion along with reflector alignment errors, followed by calibration and distortion compensation using phased array feeding techniques.

References

[1] E.J. Ruggiero and D.J. Inman, "Gossamer Spacecraft: Recent Trends in Design, Analysis, Experimentation, and Control," *Journal of Spacecraft and Rockets,* vol. 43, no. 1, Jan.–Feb. 2006, pp. 10–24.

[2] E. Im, M. Thomson, H. Fang, J.C. Pearson, J. Moore, J. Lin, "Prospects of Large Deployable Reflector Antennas for a New Generation of Geostationary Doppler Weather Radar Satellites," *AIAA Space Conf.*, Long Beach, CA, 18-20 Sept. 2007, pp. 1–11.

[3] Y. Liu, H. Du, L. Liu, J. Leng, "Shape Memory Polymers and Their Composites in Aerospace Applications: A Review," *Smart Materials and Structures,* vol. 23, 2014, pp. 1–22.

[4] R.E. Freeland, G.D. Bilyeu, and G.R. Veal, "Development of Flight Hardware for a Large Inflatable-Deployable Antenna Experiment," *Acta Astronautica*, vol. 38, Nos. 4–8, 1996, pp. 251–260.

[5] Y. Xu and F. Guan, "Structure Design and Mechanical Measurement of Inflatable Antenna, *Acta Astronautica*," vol. 76, 2012, pp. 13–25.

[6] A. Babuscia, M. Van de Loo, Q. J. Wei, S. Pan, S. Mohan, and S. Seager, "Inflatable Antenna for CubeSat: Fabrication, Deployment and Results of Experimental Tests," *2014 IEEE Aerospace Conference,* 2014, pp. 1–12.

[7] A. Babuscia, T. Choi, C. Lee, and K-M. Cheung, "Inflatable Antennas and Arrays for Interplanetary Communication Using CubeSats and SmallSats," 2015 IEEE Aerospace Conference, 2015, pp. 1–9.

[8] C.J. Wilson, "Electronically Steerable Field Reflector Techniques," Technical Report No. RADC-TR-64-521, Feb. 1965.

[9] W.D. Fitzgerald, "Limited Electronic Scanning with an Offset-Feed Near-Field Gregorian System," MIT Lincoln Laboratory Technical Report 486, 24 Sept. 1971.

[10] J.A. Martinez-Lorenzo, A. Garcia-Pino, B. Gonzalez-Valdes, and C.M. Rappaport, "Zooming and Scanning Gregorian Confocal Dual Reflector Antennas," *IEEE Trans. on Antennas and Propagat.*, vol. 56, no. 9, 2008, pp. 2910–2919.

[11] A.J. Fenn and R.J. Richardson, "Analysis of an Adaptive Two-Reflector Phased-Array Fed System," *1980 IEEE Antennas and Propagation Society International Symposium,* 2–6 June 1980, pp. 134–137.

[12] A.J. Fenn and J.W. Jordan, "Design and Analysis of an Axisymmetric Phased Array Fed Gregorian Reflector System for Limited Scanning," *2016 IEEE Int. Symp. on Phased Array Systems and Technology,* 18 – 21 October 2016, Waltham, MA, pp. 1–3.

[13] W.C. Gibson, *The Method of Moments in Electromagnetics.* Boca Raton, Florida: Chapman & Hall, 2008.

[14] J. van Tonder; U. Jakobus, "Introduction of Curvilinear Higher-Order Basis Functions for MoM and MLFMM in FEKO," *Computational Electromagnetics Workshop (CEM),* 2013, pp. 13 – 14.